A Novel Decoupling Control Method of Bearingless Permanent Magnet Synchronous Motor

Wei Du, Huangqiu Zhu and Yizhou Hua

School of Electrical and Information Engineering, Jiangsu University, Zhenjiang 212013, Jiangsu, China

Poster Session: 4.05

Post I.D. Number: Thu-Af-Po4.05-25[83]

Abstract

In this paper, a novel decoupling control method for the bearingless permanent magnet synchronous motor (BPMSM) is presented to realize the stable rotation and suspension simultaneously. The basic structure and suspension principle of the BPMSM are firstly introduced. In addition, the mathematical model of radial suspension forces and torque are established. Then, based on the reversibility analysis of the mathematical model, the adaptive fuzzy-neural network (ANFIS) is applied to construct the inverse system of the BPMSM to achieve stable operation. Finally, the research results show that the the proposed control method has good decoupling performance and stability.

Introduction

The bearingless permanent magnet synchronous motor has some remarkable advantages of simple structure, high efficiency, high torque destiny and so on. Therefore, the BPMSM has wide application prospect in some special electrical drive fields, such as precision machining, flying energy storage and extensive and aerospace fields.However, the BPMSM is a multi-variable, nonlinear system, and there is a strong coupling between the torque and suspension force of the rotor. Therefore, to realize the dynamic decoupling control is prerequisite for the steady operation of the BPMSM.

Topology of the motor

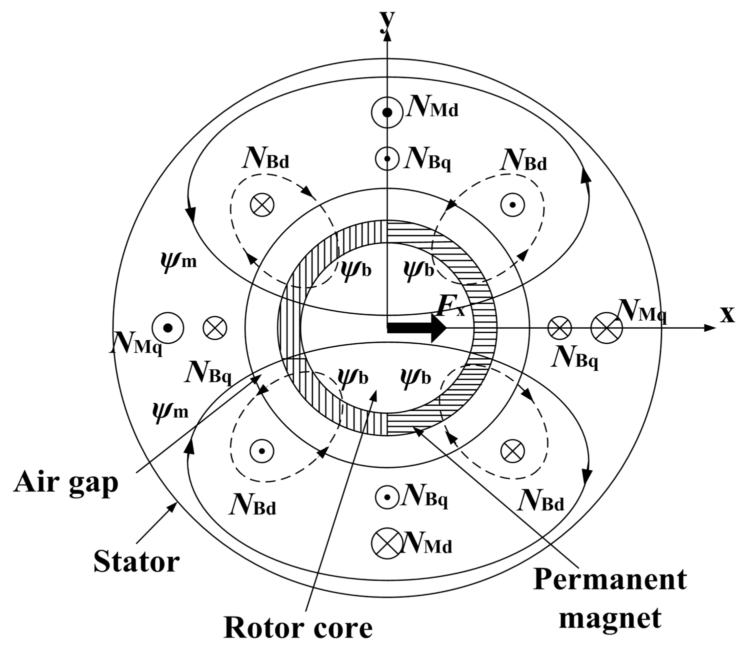

(a) suspension force generated by the suspension force windings

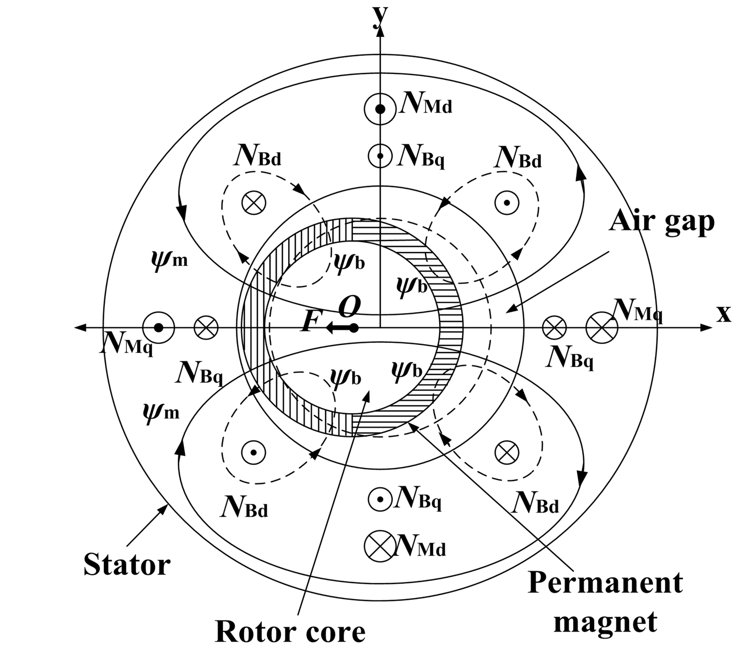

(b) magnetic pull force generated by the rotor eccentricity

- there are two sets of windings on the stator slot, where one is for torque with pole pair $P_M = 1$ and the other is for suspension force with pole pair $P_B = 2$.
- as shown in (a), when the rotor is in the centre of the motor, the flux generated by the current in the suspension force windings destroys the MFD of the torque windings and PMs, which genertes a force along the x-direction.
- as shown in (b), when the rotor has an eccentric displacement from the stator centre, the unbalance of the length of the air gap results in a single side magnetic pull force, which needs a counterforce generated by the suspension force windings to eliminate.

Methods

Mathematical model

The mathematical model of the motor includes the susepnsion force equations and the equation describingthe motion of the rotor, as follows:

$$\begin{cases} F_x = K\left(i_{Bd}\psi_{Md} + i_{Bq}\psi_{Mq}\right) + Cx \\ F_y = K\left(i_{Bq}\psi_{Md} - i_{Bd}\psi_{Mq}\right) + Cy \\ T = 3P_M\left(\psi_{Md} i_{Mq} - \psi_{Mq} i_{Md}\right)/2 \end{cases}$$

$$\begin{cases} F_x = m\ddot{x} \\ F_y - mg = m\ddot{y} \\ T - T_L = J\dot{\omega}/P_M \end{cases}$$

Analysis of inverse system

According to the interactor algorithm, $\boldsymbol{Y}=[y_1, y_2, y_3]^T=[x, y, \omega]^T$ is chosen as output variables. Meanwhile, $\boldsymbol{X}=[x_1, x_2, x_3, x_4, x_5]^T=[x, y, \dot{x}, \dot{y}, \omega]^T$, $\boldsymbol{U}=[u_1, u_2, u_3, u_4]^T=[i_{Md}, i_{Mq}, i_{Bd}, i_{Bq}]^T$ are chosen as state variables and input variables respectively. Then, to take the derivative of the output variables until it includes input variables U obviously. Finally, to calculate the rank of the Jacobi matrix.

$$\begin{cases} \dot{y}_1 = \dot{x}_1 = x_3 \\ \ddot{y}_1 = \ddot{x}_1 = \dot{x}_3 \\ \quad = \dfrac{K}{m}\left(L_{Md}u_1u_3 + \psi_f u_3 + L_{Mq}u_2u_4\right) + \dfrac{C}{m}x_1 \\ \dot{y}_2 = \dot{x}_2 = x_4 \\ \ddot{y}_2 = \ddot{x}_2 = \dot{x}_4 \\ \quad = \dfrac{K}{m}\left(L_{Md}u_1u_4 + \psi_f u_4 - L_{Mq}u_2u_3\right) + \dfrac{C}{m}x_2 - g \\ \dot{y}_3 = \dot{x}_5 = \dfrac{3}{2J}P_M^2\psi_f u_2 - \dfrac{P_M}{J}T_L \end{cases}$$

$$\boldsymbol{A}(x) = \begin{bmatrix} \dfrac{\partial\ddot{y}_1}{\partial u_1} & \dfrac{\partial\ddot{y}_1}{\partial u_2} & \dfrac{\partial\ddot{y}_1}{\partial u_3} & \dfrac{\partial\ddot{y}_1}{\partial u_4} \\ \dfrac{\partial\ddot{y}_2}{\partial u_1} & \dfrac{\partial\ddot{y}_2}{\partial u_2} & \dfrac{\partial\ddot{y}_2}{\partial u_3} & \dfrac{\partial\ddot{y}_2}{\partial u_4} \\ \dfrac{\partial\dot{y}_3}{\partial u_1} & \dfrac{\partial\dot{y}_3}{\partial u_2} & \dfrac{\partial\dot{y}_3}{\partial u_3} & \dfrac{\partial\dot{y}_3}{\partial u_4} \end{bmatrix} = \frac{K}{m}\begin{bmatrix} L_{Md}u_3 & L_{Mq}u_4 & L_{Md}u_1 + \psi_f & L_{Mq}u_2 \\ L_{Md}u_4 & -L_{Mq}u_3 & -L_{Mq}u_2 & L_{Md}u_1 + \psi_f \\ 0 & \dfrac{3m}{2JK}P_M^2\psi_f & 0 & 0 \end{bmatrix}$$

ANFIS inverse system

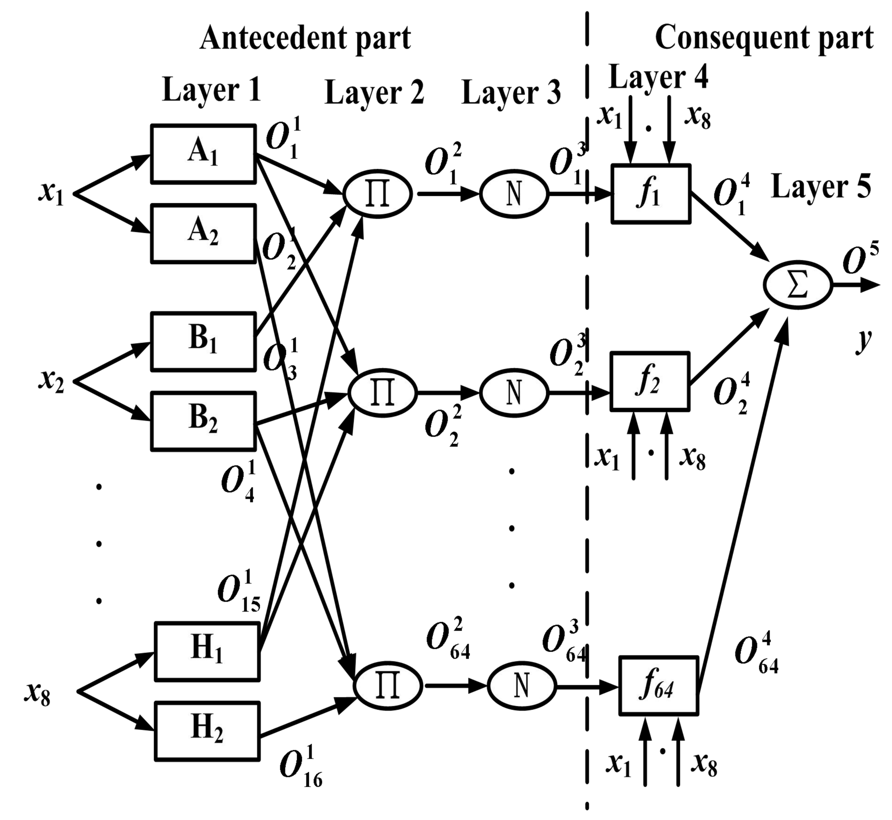

The ANFIS inverse system is based on the adaptive neuro-fuzzy inference system and it consists of the antecedent part and the consequent part, which are divided into four layers, as shown in the right figure. For each layer:

- layer 1 represents the membership function
- layer 2 is to compute the reliability of each rule
- layer 3 is to compute the normalized reliability of each rule
- layer 4 is to compute the consequent part of the rule
- layer 5 is to compute the the final output of the ANFIS

Then, to sample the date and train the ANFIS. After approximate 300 epochs, the error of ANFIS is under 0.001.

Rresluts

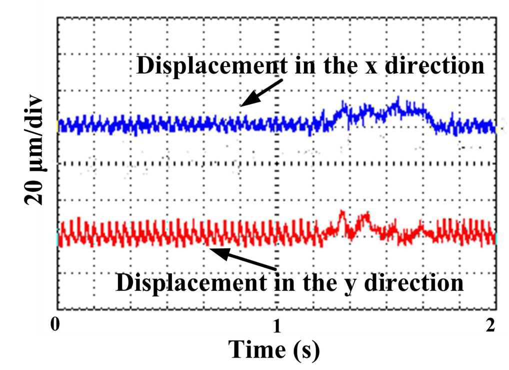

(a) Displacement waveform with direct inverse system

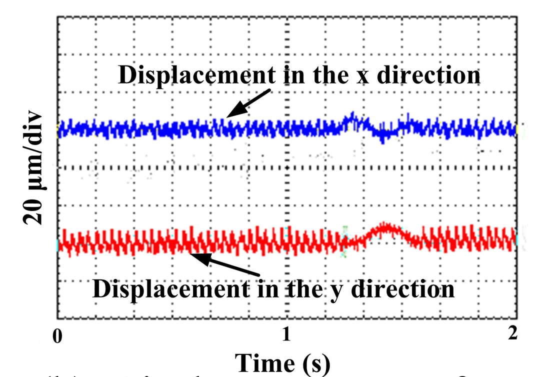

(b) Displacement waveform with ANFIS inverse system

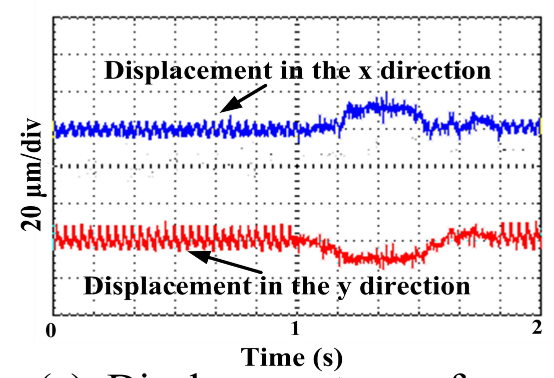

(c) Displacement waveform with direct inverse system

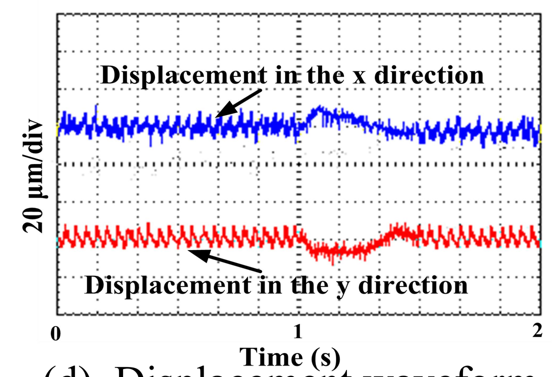

(d) Displacement waveform with ANFIS inverse system

When the speed steps from 3000 r/min to 3600 r/min, the variation of the displacement with two control methods are shown as Fig.(a) and Fig.(b). Oppositely, when the displacement with ANFIS inverse system is very small ,only about 3μm, there is strong coupling between the speed and displacement with inverse control method, the amplitude of fluctation is to about 18 μm.

When an external disturbance happens along the the gravity direction, the displacement in x-direction with ANFIS inverse system is smaller than that with inverse system, the amplitude of fluctation is decreased from about 17μm to about 10μm, which demonstrates the coupling between the displacement of x- and y-direction is weaken.

Conclusion

- A novel decoupling control method, using the ANFIS inverse system, is proposed to realize the decoupling control of the BPMSM.
- The the mathematical model of the BPMSM are introduced and an appropriate inverse system based on the ANFIS is designed to realize the decoupling control of the BPMSM.
- The comparion results of the experiments prove that the ANFIS inverse control method has better performance in decoupling control of the BPMSM, which can not only realize the decoupling control between the displacement with the speed ,but also the displacement in the x- and y-direction.

Presented at the Magnet Technology Conference , 2017 Aug. 27 – Sep.1, Amsterdam